



# Impedance-Based Out-of-Step Protection of Generator in the Presence of STATCOM

S. R. Hosseini\*, M. Karrari\*(C.A.) and H. Askarian Abyaneh\*

**Abstract:** This paper presents a novel impedance-based approach for out-of-step (OOS) protection of a synchronous generator. The most popular and commonly used approaches for detecting OOS conditions are based on the measurement of positive sequence impedance at relay location. However, FACTS devices change the measured impedance value and thus disrupt the performance of impedance-based relay function. In this paper, the performance of synchronous generator OOS protection function connected to the transmission line in the presence of a static synchronous compensator (STATCOM) is investigated. Moreover, an analytical adaptive approach is used to eliminate the effect of STATCOM. This approach requires only the remote bus voltage and current phasors to be sent to the relay location via a communication channel. Simulation results show that STATCOM changes impedance trajectory and causes the incorrect operation of OOS relay. Furthermore, the proposed approach corrects the relay mal-operation and improves the accuracy of OOS impedance-based function when the STATCOM is used in the system.

**Keywords:** Out-of-Step Protection, STATCOM, Impedance Trajectory, Synchronous Generator.

## 1 Introduction

**D**ISTURBANCES in power systems such as faults, line switching, and generator outage lead to electro-mechanical oscillations and power swing. In the unstable case of oscillations, severe disturbances may cause a large deviation of generator rotor angles, and the generator loses its ability to operate synchronously with the power system grid. This condition is called out-of-step (OOS). During OOS condition, there are large cyclic variations in the currents and voltages of the effected machine. These stresses are detrimental to not only the affected generator but also it may endanger the stability of the entire system [1, 2].

To avoid such damages, a reliable generator protection scheme is necessary to detect the OOS condition. Until now, many techniques have been proposed to detect the OOS condition. Conventional

impedance-based techniques detect the OOS condition by analyzing the measured impedance at the R-X plane [3, 4]. Recent studies have presented new approaches such as the equal area criterion (EAC), extended equal area criterion (EEAC), swing center voltage, and distributed dynamic state estimator [5-10]. The main features of these methods are compatibility and strength against changes in power system configuration. However, these approaches are complicated, difficult to implement and need at least the instance of fault clearing time to be fed as an input to the relay [2]. Therefore, impedance-based techniques are still incorporated for OOS condition detection.

In recent years, FACTS controllers have been used in transmission lines for different purposes such as reactive power control, voltage profile correction, increasing transmission line capacity, and improving the dynamic/transient stability of power systems [11]. In spite of all advantages, these devices change the voltage and current of the network and cause the mal-operation of impedance-based protective relays [12]. Many studies have examined the effect of FACTS devices on distance protection [13-22]. Results show that the presence of various series and shunt controllers usually makes distance relays under-reach, thereby changing trip characteristic of the distance relay [14].

Iranian Journal of Electrical and Electronic Engineering, 2019.

Paper first received 10 March 2019 and accepted 05 June 2019.

\* The authors are with the Aboorayhan Building, Department of Electrical Engineering, Amirkabir University of Technology, Tehran, Iran.

E-mails: [sr.hosseini@aut.ac.ir](mailto:sr.hosseini@aut.ac.ir), [karrari@aut.ac.ir](mailto:karrari@aut.ac.ir), and [askarian@aut.ac.ir](mailto:askarian@aut.ac.ir).

Corresponding Author: M. Karrari.

Other studies have investigated the effects of FACTS devices on the loss-of-excitation (LOE) protection of synchronous generators [22-26]. Results revealed that the presence of FACTS causes a substantial delay in the performance of LOE relay.

Discrimination of power swing and fault condition in transmission lines is done by distance relays. But in the power plants the power swing is detected by OOS function. In spite of extensive research on the performance of distance relays in the presence of FACTS devices only a few articles have been published on distance relay performance for a compensated line during the power swing condition [27-31]. In [27, 28] various methods for discriminating the power swing from a fault were presented in a fixed capacitor compensated line. Moravej *et al.* studied the impact of UPFC on swing characteristics and it is shown that parameters of transmission line (ABCD) would change in the presence of UPFC [29]. The effect of SSSC on the locus of the apparent impedance under different system operation and fault condition is studied by Jamali in [30]. The Performance of power swing blocking methods in compensated transmission line by UPFC was investigated by Khodaparast *et al.* in [31]. Despite studies to investigate the effect of FACTS devices on the distance relay under Power swing conditions, no study has examined the effect of FACTS devices on synchronous generator OOS protection.

In this paper, the impact of STATCOM on the performance of OOS protection has been investigated. Impedance-based OOS protection detects the OOS condition by comparing the measured impedance with supervisory characteristic at the R-X plane. Unlike distance relays, the rate of change of impedance does not apply to OOS diagnosis. Due to the widespread use of impedance-based relay for detecting OOS condition, it is essential to consider the effect of FACTS devices on this protection function. Contributions of this paper are as follows:

1. The dynamic response of STATCOM has been studied during OOS condition in the presence and absence of STATCOM.
2. Full detailed modeling of STATCOM in two modes (reactive power control and voltage regulation operation) is simulated and the effect of STATCOM on the performance of the OOS relay has been investigated.
3. An analytical approach is developed to eliminate the negative effect of STATCOM on measured impedance by the OOS relay. This approach uses the voltage and current phasor information sampled by PMU in the remote bus of the generator.

**2 Conventional Impedance-Based OOS Protection**

**2.1 Behavior of Impedance Trajectory during Swing**

The OOS condition in synchronous generators can be

illustrated by considering the simple two-machine system in Fig. 1. This system consists of a generator connected to an infinite bus by a step-up transformer and transmission line.  $E_A$  and  $E_B$  are the amplitude of generator internal voltage and external system voltage, respectively. Angle  $\delta$  is the phase angle of generator internal voltage phasor that equals to generator rotor angle.  $Z_g$ ,  $Z_{tr}$ ,  $Z_{line}$  and  $Z_e$  denote the generator, transformer, transmission line, and external system impedances, respectively. The effect of rotor angle swings on the relay quantities is analyzed by considering the measured impedance by relay installed at the generator terminal (Bus C).

The measured impedance by the OOS relay can be found as follows:

$$Z_R = \frac{\tilde{V}_t}{\tilde{I}_t} = \frac{E_A \angle \delta - Z_g \tilde{I}_t}{\tilde{I}_t} \tag{1}$$

where,  $\tilde{V}_t$  and  $\tilde{I}_t$  are terminal voltage and current, respectively.  $\tilde{I}_t$  can be written as (2).

$$\tilde{I}_t = \frac{E_A \angle \delta - E_B \angle 0}{Z_{tot}} \tag{2}$$

By substituting (2) into (1), the measured impedance by OOS relay can be written as follows:

$$Z_R = -Z_g + Z_{tot} \frac{E_A \angle \delta}{E_A \angle \delta - E_B \angle 0} \tag{3}$$

where,  $Z_R$  is the measured impedance and  $Z_{tot}$  as shown in Fig. 1, is the sum of the impedances between  $E_A$  and

$E_B$ . If  $K = \frac{E_A}{E_B}$  is defined, then the measured impedance

is obtained with some calculations as follows:

$$Z_R = -Z_g - \frac{Z_{tot}}{1 - \frac{1}{K} e^{-j\delta}} \tag{4}$$

Based on (4), the measured impedance is a function of  $\delta$  and voltage amplitude ratio ( $K$ ). Furthermore, this result is valid for single-machine system in which the generator is connected to an infinite bus by the transmission line. Fig. 2 shows the locus of measured impedance  $Z_R$  as a function of  $\delta$  for different values of  $K$  on an R-X diagram [1]. If  $K = 1$ , the impedance path perpendicularly passes from the center of the system impedance line. The angle between any point of the

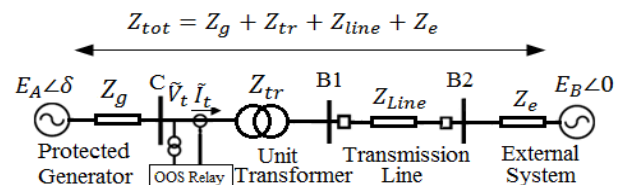


**Fig. 1** The two-machine system.

locus and points A and B is equal to the corresponding  $\delta$ . At the middle of system impedance line,  $\delta = 180^\circ$ . This point is called electrical center of system and the voltage at this point is equal to zero. Therefore, in this point the relay will witness a three phase fault at the electrical center point and a high-current is drawn from the generator. If  $K \neq 1$ , the impedance loci are circles with their centers on the extensions of impedance line AB. For  $K > 1$ , the electrical center will be above the impedance center and if  $K < 1$ , the electrical center will be below the impedance center. The electrical centers are not fixed points since the effective machine reactance and the magnitudes of internal voltage vary during dynamic conditions [1].

During an OOS condition, the impedance locus moves on the circles, and the rotor angle oscillates between  $-180^\circ$  and  $180^\circ$ . These oscillations lead to cyclic variations in the currents and voltage of the affected machine, with frequency being a function of the rate of slip of its poles. The high-amplitude currents and off-nominal frequency operation could result in winding stresses and pulsating torques that can excite potentially damaging mechanical vibrations. There is also a risk of losing the stability of the whole system when several units are simultaneously oscillating in two or more coherent groups.

**2.2 Generator OOS Protection**

In the case of the electrical center is placed inside the transmission system, the detection of OOS condition and isolation of the unstable generator are accomplished by line protection. However, for situations where the electrical center is within the generator or step-up transformer, a special relay must be provided at the generator. Such a situation occurs when a generator pulls out of synchronism in a system with strong transmission. A low excitation level on the generator ( $E_A < E_B$ ) also tends to contribute to such a condition.

In order to prevent destructive effects on the units and maintain system stability, it is desirable to have an OOS

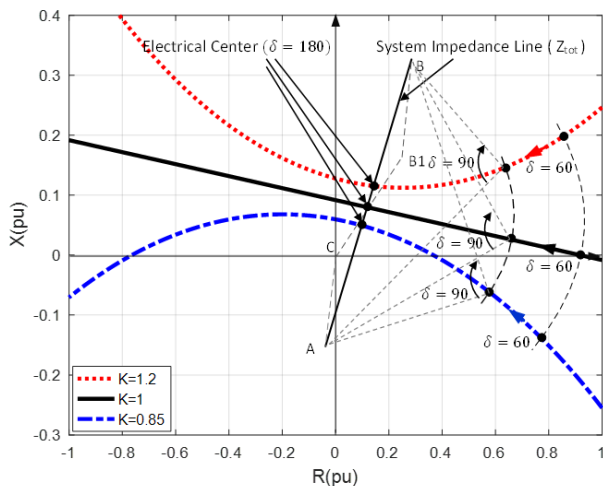


Fig. 2 Impedance trajectory.

relay that will trip the unit. Tripping should be restricted to the disconnection of the machine from the system by opening the generator circuit breaker rather than initiating a complete shutdown of the unit. This allows the resynchronization of the generator as soon as conditions stabilize. Two commonly used approaches to generator OOS protection are the mho element and the blinder scheme [1]. In this study, we used the blinder scheme presented in [32].

**2.2.1 Blinder Scheme Principle**

This scheme consists of two impedance elements, referred to as blinders, and a supervisory relay with an offset mho characteristic (see Fig. 3(a)) [1].

Reference [27] used the blinder scheme to implement the OOS protection function. Fig. 3(b) illustrates the characteristic of this function which consists of two polygons. Characteristic 1 represents the lower section of the rectangle and Characteristic 2 covers the upper hatched area. Depending on the electrical center of the power swing, or in the vicinity of the power station, the impedance trajectory passes through the range of Characteristic 1 or that of Characteristic 2. The intersection point of the imaginary axis and the impedance trajectory assign the characteristic for relay operation. Characteristic boundaries are determined by the setting parameter impedances  $Z_a, Z_b, Z_c$  and  $(Z_d - Z_c)$  which are given in Table 1. The polygon is symmetrical around its vertical axis. In Fig. 3(b), the diagnosis of OOS condition requires that the impedance trajectory enter a characteristic side and exit the opposite side (Cases 1 and 2). On the other hand, if the impedance trajectory enters and exits the same side, the power swing will tend to stabilize (Cases 3 and 4).

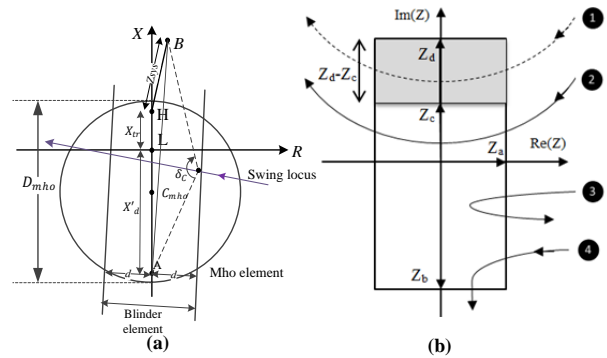


Fig. 3 Generator OOS protection using a blinder scheme.

Table 1 Setting parameters of OOS relay polygon.

Parameter	Setting
$Z_a$	$Z_a \approx \frac{x'_d + X_{TR} + X_{sys}}{2 \tan(\delta_{CRIT} / 2)}$ & $\delta_{CRIT} = 120$
$Z_b$	$x'$
$Z_c$	$(0.7-0.9) X_{tr}$
$Z_d$	$X_{tr} + \alpha X_{sys}$ & $\alpha \approx 0.25-0.30$

### 3 Impedance-Based OOS Protection Function

Fig. 4 illustrates the simplified single-line diagram of the power system introduced in Fig. 1. This system consists of a synchronous generator connected to an infinite bus by the transmission line.  $Z_1$  is equal to  $Z_g$ ,  $Z_{tr}$  is step up transformer impedance and  $Z_2$  is equal to the transmission line impedance. Before the installation of the STATCOM, the impedance measured by OOS relay can be found by Eqs. (5)-(7).

$$\tilde{I}_R = \frac{\tilde{E}_1 - \tilde{E}_2}{Z_1 + Z_{tr} + Z_2} \quad (5)$$

$$\tilde{V}_R = \tilde{E}_1 - Z_1 \tilde{I}_R \quad (6)$$

$$Z_R = \frac{\tilde{V}_R}{\tilde{I}_R} = \frac{\tilde{E}_1(Z_2 + Z_{tr}) + \tilde{E}_2 Z_1}{\tilde{E}_1 - \tilde{E}_2} \quad (7)$$

In this equations,  $\tilde{E}_1$  and  $\tilde{E}_2$  represent the generator internal voltage and remote bus voltage phasors, respectively. The phasors  $\tilde{V}_R$  and  $\tilde{I}_R$  are the voltage and current measured at the generator terminal bus.

Now suppose a shunt STATCOM is connected to the system at the beginning of the transmission line (see Fig. 5(a)). STATCOM is a shunt device of the FACTS family using power electronics to control reactive power and improve transient stability on power grids [11]. The STATCOM regulates voltage at its terminal by controlling the amount of reactive power injected into or absorbed from the power system.

The equivalent circuit of the right side of B2 busbar can be considered as thevenin equivalent circuit (see

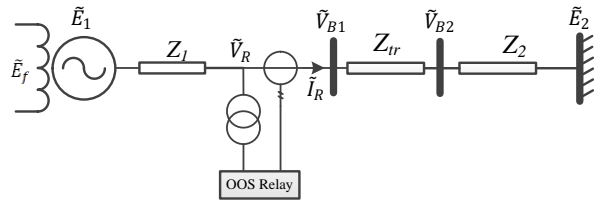


Fig. 4 Single-line diagram of the studied power system.

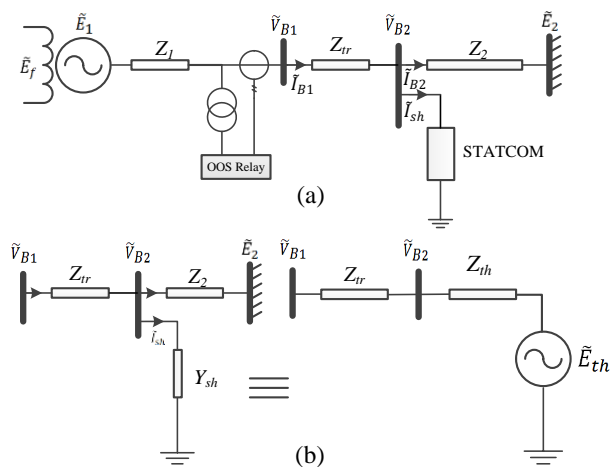


Fig. 5 a) Equivalent circuit of the network side of Fig. 4, b) Equivalent network after installing STATCOM.

Fig. 5(b)). This equivalent circuit is similar to the original system before installing of STATCOM with the difference that the impedance  $Z_2$  and voltage  $\tilde{E}_2$  have been replaced by thevenin impedance ( $Z_{th}$ ) and voltage ( $\tilde{E}_{th}$ ). Therefore, by having the thevenin values, the measured impedance is obtained by (7).

In Fig. 5(b), thevenin impedance and voltage can be calculated by (8) and (9), respectively.

$$Z_{th} = Z_2 \parallel Y_{sh} = \frac{Z_2}{1 + Z_2 Y_{sh}} \quad \& \quad Y_{sh} = \frac{\tilde{I}_{sh}}{\tilde{V}_{B2}} \quad (8)$$

$$\tilde{E}_{th} = \frac{1}{1 + Z_2 Y_{sh}} \tilde{E}_2 \quad (9)$$

In these equations  $Y_{sh}$ ,  $\tilde{V}_{B2}$ , and  $\tilde{I}_{sh}$  are the equivalent admittance, voltage and current of the STATCOM, respectively. The STATCOM is modelled as time varying impedance and its value should be calculated at any time step. The phasors  $\tilde{V}_{B2}$  and  $\tilde{I}_{sh}$  are calculated according to (10) and (11), respectively.

$$\tilde{V}_{B2} = \tilde{V}_{B1} - Z_{tr} \tilde{I}_{B1} \quad (10)$$

$$\tilde{I}_{sh} = \tilde{I}_{B1} - \tilde{I}_{B2} \quad (11)$$

By comparing the equivalent thevenin circuit by original system the measured impedance by OOS relay can be written as follows:

$$Z_R = \frac{\tilde{V}_R}{\tilde{I}_R} = \frac{\tilde{E}_1(Z_{tr} + Z_{th}) + \tilde{E}_{th} Z_1}{\tilde{E}_1 - \tilde{E}_{th}} \quad (12)$$

Based on (12), by installing the STATCOM on the network, the value of impedance is changed and may lead to mal-operation of the relay.

#### 3.1 Modified Adaptive OOS Protection

To eliminate the effect of STATCOM on measured impedance, thevenin equivalent values from (8) and (9) must be substituted into (12). Thus we will have:

$$\begin{aligned} Z_R &= \frac{\tilde{E}_1 \left( Z_{tr} + \frac{Z_2}{1 + Z_2 Y_{sh}} \right) + \left( \frac{1}{1 + Z_2 Y_{sh}} \tilde{E}_2 \right) Z_1}{\tilde{E}_1 - \left( \frac{1}{1 + Z_2 Y_{sh}} \tilde{E}_2 \right)} \\ &= \frac{\tilde{E}_1 (Z_{tr} + Z_{tr} Z_2 Y_{sh} + Z_2) + \tilde{E}_2 Z_1}{(1 + Z_2 Y_{sh}) \tilde{E}_1 - \tilde{E}_2} \\ &= \frac{\tilde{E}_1 (Z_{tr} + Z_2) + \tilde{E}_2 Z_1}{(1 + Z_2 Y_{sh}) \tilde{E}_1 - \tilde{E}_2} + \frac{Z_{tr} Z_2 Y_{sh} \tilde{E}_1}{(1 + Z_2 Y_{sh}) \tilde{E}_1 - \tilde{E}_2} \\ &= \frac{\tilde{E}_1 (Z_{tr} + Z_2) + \tilde{E}_2 Z_1}{(1 + Z_2 Y_{sh}) \tilde{E}_1 - \tilde{E}_2} \times \frac{\tilde{E}_1 - \tilde{E}_2}{\tilde{E}_1 - \tilde{E}_2} + \frac{Z_{tr} Z_2 Y_{sh} \tilde{E}_1}{(1 + Z_2 Y_{sh}) \tilde{E}_1 - \tilde{E}_2} \Rightarrow \\ Z_R &= Z_R^0 \times \frac{\tilde{E}_1 - \tilde{E}_2}{(1 + Z_2 Y_{sh}) \tilde{E}_1 - \tilde{E}_2} + \frac{Z_{tr} Z_2 Y_{sh} \tilde{E}_1}{(1 + Z_2 Y_{sh}) \tilde{E}_1 - \tilde{E}_2} \quad (13) \end{aligned}$$

By some manipulations, the modified impedance is

obtained as follows:

$$Z_R^0 = Z_R + (Z_R - Z_{ir})Z_2Y_{sh} \frac{\tilde{E}_1}{\tilde{E}_1 - \tilde{E}_2} \quad (14)$$

In this equation,  $Z_R$  is the measured impedance by relay and  $Z_R^0$  is the modified impedance. In general, with installation of STATCOM at  $m$  percent distance from the beginning of transmission line, the thevenin equivalent parameters are obtained by (15) and (16), respectively.

$$Z_{th} = (1-m)Z_2 \parallel Y_{sh} = \frac{(1-m)Z_2}{1+(1-m)Z_2Y_{sh}} \quad (15)$$

$$\tilde{E}_{th} = \frac{1}{1+(1-m)Z_2Y_{sh}} \tilde{E}_2 \quad (16)$$

If the similar calculations for  $Z_R^0$  are repeated with the corresponding thevenin voltage and impedance values with  $m \neq 0$ , the modified impedance will be as follows:

$$Z_R^0 = Z_R + (Z_R - Z_{ir} - mZ_2) \times (1-m)Z_2Y_{sh} \frac{\tilde{E}_1}{\tilde{E}_1 - \tilde{E}_2} \quad (17)$$

It should be noted that the modified impedance value in (14) and (17) is not exactly the same as measured impedance before installing the STATCOM. Because the voltage phasors  $\tilde{E}_1$  and  $\tilde{E}_2$  are changed by installing the STATCOM. Another point to be considered is that this modification only requires one remote bus or STATCOM voltage and current phasors samples to be sent generator terminal. Similarly, remote data transfer to the relay location for other protection functions are also proposed in the literatures. For example, in order to modify the LOE function, the algorithms presented in [24, 26] require sending the FACTS devices data to the relay location. Also, double-ended fault location algorithms need remote bus data [33]. Therefore, for implementation of some protection function, remote signal system is needed. Nowadays, this possibility is provided by using phasor measurement units (PMUs) on the network.

The internal voltage of synchronous generator is calculated by the voltage and current phasors measured at relay location. The direct method for calculating the internal voltage phasor is presented in the next section.

### 3.2 Direct Method for Internal Voltage Phasor Calculations

The internal voltage phasor can be calculated using KVL at generator terminal. Fig. 6 represents the voltage phasor diagram of the machine. According to Fig. 6, the internal voltage phasor is calculated as follows [1]:

$$\tilde{E}_q = |\tilde{E}_q| \angle \theta = \tilde{V}_t + (R_a + jX_q) \tilde{I}_t \quad (18)$$

where,  $\theta$  is the angle of internal voltage vector referring to the terminal voltage vector. The rotor angle is the angle of internal voltage referring to the reference bus. Therefore, to gather the rotor angle, the angle of generator terminal voltage ( $\alpha$ ) must be added to  $\theta$  (Fig. 6).

$$\delta = \theta + \alpha \quad (19)$$

Equation (18) is valid for the steady state condition. However, since the rotor angle stability and OOS condition are low frequency phenomena, (18) is valid during the receiving data window and can be used in this study. Fig. 7 shows the comparison of real and calculated rotor angles of generator in the single-machine infinite bus (SMIB) test system shown in Fig. 8. Detail information of this system is presented in example 13.2 of [1]. After the occurrence of a three phase fault at point F in the transmission line, the rotor angle oscillates. The fault occurs at  $t=1$ sec and duration of fault is 0.06 sec, i.e., less than the critical clearing time of the generator. It is clear that the calculated angle is almost equal to the real angle in post fault duration.

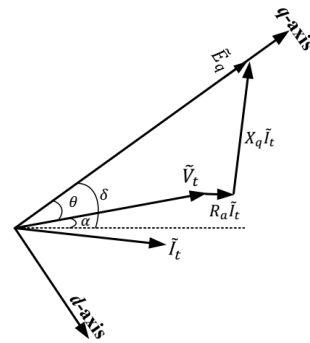


Fig. 6 Voltage phasor diagram of the two-machine system.

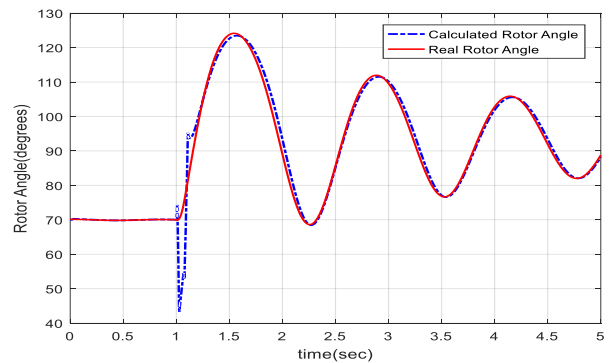


Fig. 7 Comparison of real and calculated rotor angles of the generator.

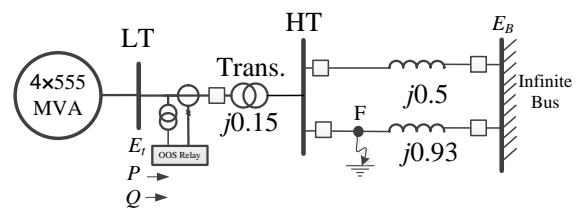


Fig. 8 Single-machine infinite bus system.

**4 Performance of Modified OOS Function in the Presence of STATCOM**

To investigate the effect of STATCOM on OOS relay function, the SMIB test system presented in [1] is used. As shown in Fig. 8, the system consists of four 555 MVA synchronous machines that are modelled with an equivalent generator. This equivalent generator is connected to the infinite bus through the step-up transformer and the double-circuit transmission line. The simulation studies have been carried out in the MATLAB/Simulink environment. The system nominal frequency is 60 Hz. Other detail information about this system is presented in Appendix 1. In practice, to protect the generator, the voltage and current are sampled at generator terminal and before the step-up transformer. In this study, the samples also were taken in the LT bus before the step up transformer while in [1] sampling was done in the HT bus after the step up transformer.

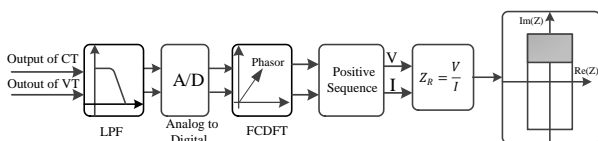
**4.1 Impedance Trajectory**

Fig. 9 depicts the block diagram of the impedance-based OOS relay. First, the voltage and current are sampled by voltage and current transformers. Then, the samples pass through the low-pass filter (LPF) to remove high-frequency components. The cut off frequency of LPF is set 120 Hz. By sampling voltage and current real time signals analogue-to-digital conversion is done. The sampling frequency must be at least ten times greater than network frequency to reflect the system dynamics. In this study, the sampling frequency is considered 25 kHz. In the next step, voltage and current phasors are calculated by full-cycle discrete Fourier transform (FCDFT). The Fourier block performs a Fourier analysis of the input signal over a running window of one cycle of the fundamental frequency of the signal. The detail about phasor calculation is presented in the next subsection. The measured apparent impedance is obtained by voltage-to-current phasors ratio. Finally, the impedance trajectory is obtained by plotting the apparent impedance on the real-image plane.

**4.1.1 Phasor calculation**

The Fourier analysis is used to calculate voltage and current phasors calculation. Recall that a signal  $f(t)$  can be expressed by a Fourier series of the form (20).

$$f(t) = \frac{a_0}{2} + \sum_{n=1}^{\infty} a_n \cos(n\omega t) + b_n \sin(n\omega t) \tag{20}$$



**Fig. 9** OOS relay block diagram.

$$a_n = \frac{2}{T} \int_{t-T}^t f(t) \cos(n\omega t) dt \tag{21}$$

$$b_n = \frac{2}{T} \int_{t-T}^t f(t) \sin(n\omega t) dt \tag{22}$$

where,  $T = 1/f_1$  and  $f_1$  is the fundamental frequency of signal in Hz and also  $\omega = 2\pi f_1$  is the fundamental frequency is rad/sec.

In (20)-(22),  $n$  represents the rank of the harmonics. ( $n = 1$  corresponds to the fundamental component.) The magnitude and phase of the selected harmonic component are calculated by these equations:

$$|H_n| = \sqrt{a_n^2 + b_n^2} \tag{23}$$

$$\angle H_n = \tan^{-1} \left( \frac{b_n}{a_n} \right) \tag{24}$$

The positive sequence voltage and current phasors, is calculated based on (21)-(24) for  $n = 1$ .

**4.1.2 Fault Scenario**

A three-phase short circuit fault occurred at the beginning of the second line (Point F) at time  $t = 1$  sec, and the second line is disconnected from the network at  $t = 1.1$  sec. After the fault is cleared, the generator accelerates and the  $\delta$  angle increases. This situation causes the impedance path move to the left side and leaves from the left side of Characteristic 2. The impedance path between time interval  $t = 1.11$  sec to  $t = 1.72$  sec, is illustrated in Fig. 10 that is identical with the result of Example 13.6 presented in [1]. The rotor angle variations during and after fault interval demonstrated in Fig. 11. It is evident that, after the clearing fault, the rotor angle is not stable and fluctuates between  $180^\circ$  and  $-180^\circ$ .

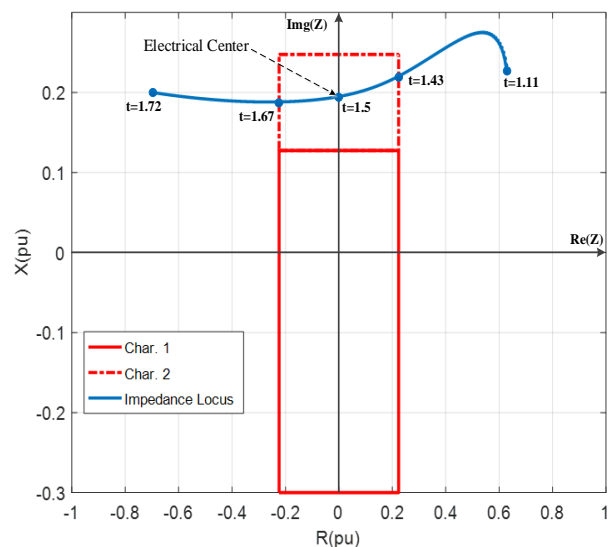


**Fig. 10** Impedance locus after fault in time interval  $t = 1.11$  sec to  $t = 1.72$  sec.

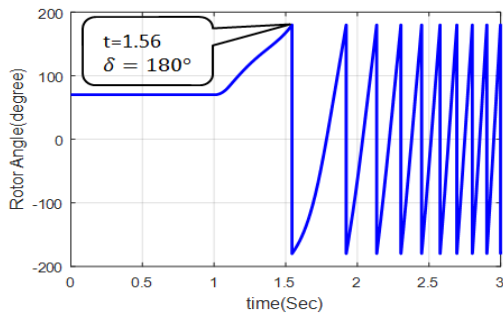


Fig. 11 The rotor angle variations during OOS condition.

**4.2 The Effect of STATCOM on the Impedance Trajectory**

To examine the effect of STATCOM on the measured impedance by OOS relay, a  $\pm 200$  MVar STATCOM is installed at the HT bus of SMIB system. It consists of a GTO-based, square-wave, 48-pulse voltage-sourced converter (VSC) and interconnection transformers for harmonic neutralization. During the fault, the dynamic of STATCOM is comparable relative to the transients and phasor modeling of STATCOM leads to erroneous results. Therefore, detailed (discrete) modeling of the STATCOM is required.

The VSC is made up by cascading four 12-pulse three-level inverters and two series-connected capacitors which acts similarly to a variable DC voltage source in the DC bus of the converter. Detailed parameters of the STATCOM are given in Appendix 2 and more information such as component interconnection and control system topology are reported in [11].

During fault condition, the STATCOM can improve transient stability through reactive power injections into the short circuit point. Due to the rapid response of the STATCOM, this equipment has a significant impact on the transient stability of the power system and increases critical fault clearing time [11]. However, it may interfere with the operation of the OOS relay. On the other hand, if the fault duration is less than the critical fault clearing time, the STATCOM makes the generator to be stable. Otherwise, the generator will be unstable and the relay operation may be disrupted.

Fig.12 shows the measured impedance trajectory after the occurrence of short circuit when the STATCOM is in service. The STATCOM is simulated in the two modes of voltage regulation (VR) and Q-control (QC). To create unstable conditions, the fault lasts for 0.03 sec more than the critical clearing time. In Table 2, the corresponding times are given with and without STATCOM. In this table, important times are compared and 'ND' stands for Not Detected. According to Fig. 12, it is clear that the STATCOM changes the impedance path and causes it to exit from the upper side of the polygon. In both QC and VR modes, impedance trajectory enters from right side of Characteristic 2, but does not have any intersection with imaginary axis

inside the Characteristics 1 and 2. Therefore, in both modes, the OOS will not be detected. On the other hand, the STATCOM causes the electrical center to move away from the generator which it leads to relay mal-operation. The next rounds impedance trajectory in the QC mode is illustrated in Fig. 13. It is clear that the exit point of impedance trajectory also leaves from the upper side of Characteristic 2. In the VR mode, the impedance trajectory is almost the same and exits from the upper side of Characteristic 2; repetition is avoided.

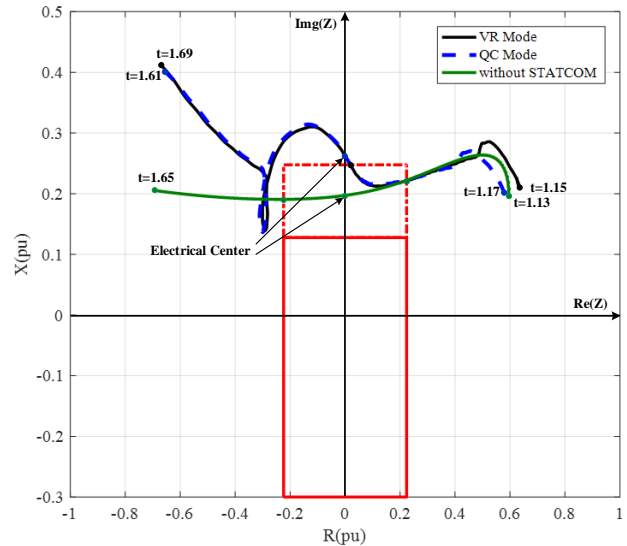


Fig. 12 Impedance trajectory after installing the STATCOM.

Table 2 Comparison of important OOS relay times.

	Without STATCOM	With STATCOM	
		VR Mode	QC Mode
Critical clearing Time( $t_c$ [sec])	0.07	0.082	0.0989
Fault Clearing Time ( $t_{clear}$ [sec])	1.1	1.112	1.1289
Characteristic Entering Time ( $t_{en}$ [sec])	1.43	1.41	1.36
Characteristic Outing Time ( $t_{out}$ [sec])	1.67	1.55	1.48
$t_{\delta = 180}$ [sec]	1.5	1.555	1.485
Detection Time [sec]	0.67	ND	ND

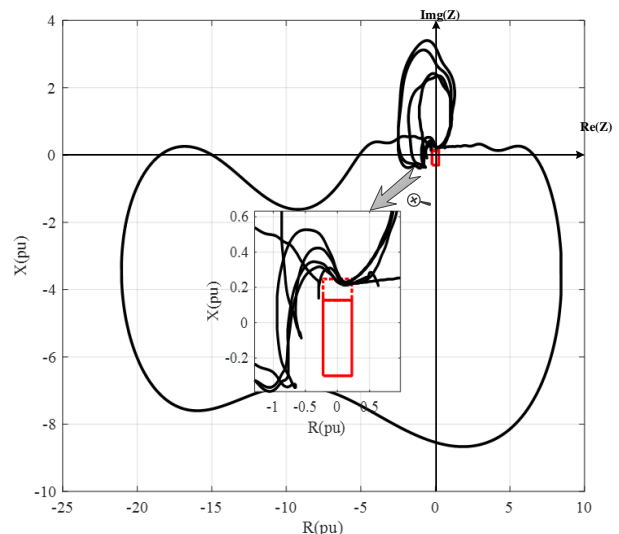


Fig. 13 Next rounds of the impedance trajectory in the presence of STATCOM.

The relay operation is examined by the presence of STATCOM in the middle of the transmission lines. Fig. 14 shows the SMIB system with the STATCOM installed in the middle of the transmission lines. Simulation results of the OOS relay operation following the tree phase fault in points F1 to F4 are given in Table 3. In all cases, F1 to F4, the three-phase error lasted for 0.02 sec more than the critical clearing time of system with the STATCOM and then the breakers of faulted line open. These results show that the presence of middle STATCOM has less effect on OOS relay operation and it only causes delay time on relay operation.

### 4.3 Evaluation of the Modified Relay Function

The modified OOS relay function block diagram is

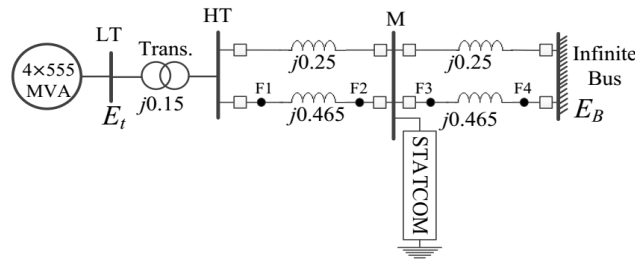


Fig. 14 Single-machine infinite bus test system with the middle STATCOM.

Table 3 OOS relay operation times for middle STATCOM.

Fault Location	$t_c$ [sec]		Detection Time [sec]		Delay [sec]
	Without STATCOM	With STATCOM	Without STATCOM	With STATCOM	
F1	1.067	1.075	1.7	1.75	0.05
	$t_{clear} = 1.095$				
F2	1.036	1.080	1.803	1.806	0.003
	$t_{clear} = 1.100$				
F3	1.033	1.049	1.82	1.823	0.003
	$t_{clear} = 1.069$				
F4	1.12	1.15	2.2	2.72	0.52
	$t_{clear} = 1.170$				

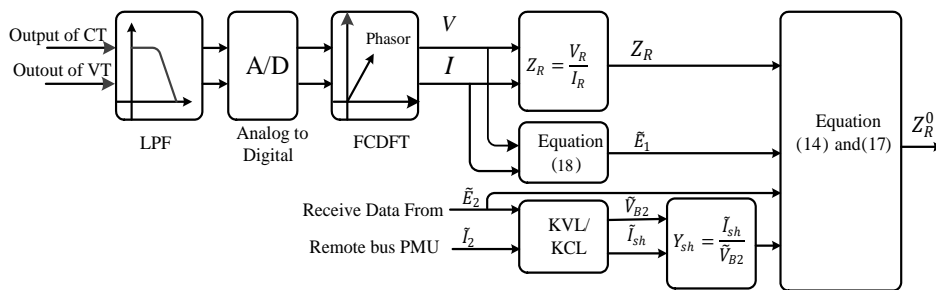


Fig. 15 The modified OOS relay block diagram.

Table 4 Comparison of important times of Modified OOS relay.

	Without STATCOM	With STATCOM	
		VR Mode	QC Mode
Critical Clearing Time ( $t_c$ )	0.07	0.082	0.0989
Fault Clearing Time ( $t_{clear}$ )	1.1	1.112	1.1289
Characteristic Entering Time ( $t_{en}$ [sec])	1.43	1.19	1.23
Characteristic Outing Time ( $t_{out}$ [sec])	1.67	1.45	1.542
$t_{\delta=180}$ [sec]	1.5	1.347	1.375
Detection Time [sec]	0.67	0.45	0.542

installed at the HT bus of SMIB system in Fig. 8. By applying the modifications process presented in Fig. 15, simulations are repeated at the same fault clearing time of Table 2. The comparison of important times for modified OOS relay are given in Table 4. Based on Table 4, the relay detects OOS condition correctly using the modified algorithm.

The results show that the relay detects the OOS condition after 0.45 sec and 0.542 sec, respectively, in VR and QC modes. The detection time of different cases with and without STATCOM in different modes cannot be compared together. Because the critical fault clearing time is different and, therefore, the fault duration time varies. Detection time is faster in VR mode than the QC mode, which is also faster than the case without STATCOM. In other words, after a fault occurs, the STATCOM in both VR and QC modes starts injecting reactive power into the faulted point and tries to regulate the voltage of the connected point. If the power of STATCOM is sufficient and the fault duration is short, these actions maintain the stability of the system; otherwise, they lead to incorrect detection. Based on Fig. 16, in the VR operation mode, the modified impedance path enters the right side of Characteristic 2 and leaves the left side. Because of the oscillating nature of the OOS, the impedance trajectory rotates in closed paths and re-enters the characteristic and leaves it. Fig. 17 shows the second intersection of impedance path with Characteristic 2. It is obvious that the relay is robust for the following turns and operates correctly.

Similar results are obtained when the STATCOM is operated in the QC mode. Fig. 18 demonstrates the modified impedance trajectory at this operation mode. After 0.1289 sec of fault duration, the relay detects OOS after 0.542 sec. The second turn of the impedance trajectory crosses the left side of Characteristic 2 after

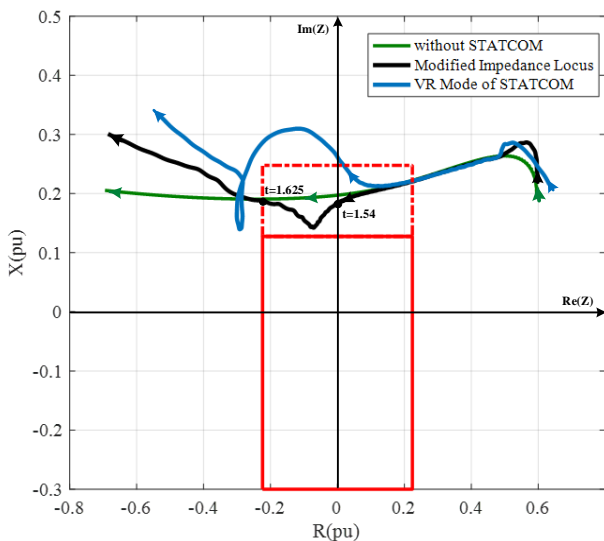


Fig. 16 The modified impedance trajectory with STATCOM in the VR mode.

1.83 sec. The next turns are not perfect circles because of the change in voltage and voltage ratio (K) by the STATCOM.

The modified OOS relay works correctly for the diagnosis of stable oscillations and during stable power swing. In these situations, the impedance trajectory does not enter Characteristics 1 or 2. An example of modified impedance trajectory in the stable conditions is shown Fig. 19. In Fig. 19 the STATCOM was operated in QC mode and the fault duration was 0.06 sec that is less than the critical clearing time in this mode. It is clear that the impedance trajectory has not entered in the characteristics and the swing is detected stable. The rotor angle variations are illustrated in Fig. 20. It is clear that the oscillations are gradually reduced and the system is stable.

The approach presented in this paper can be

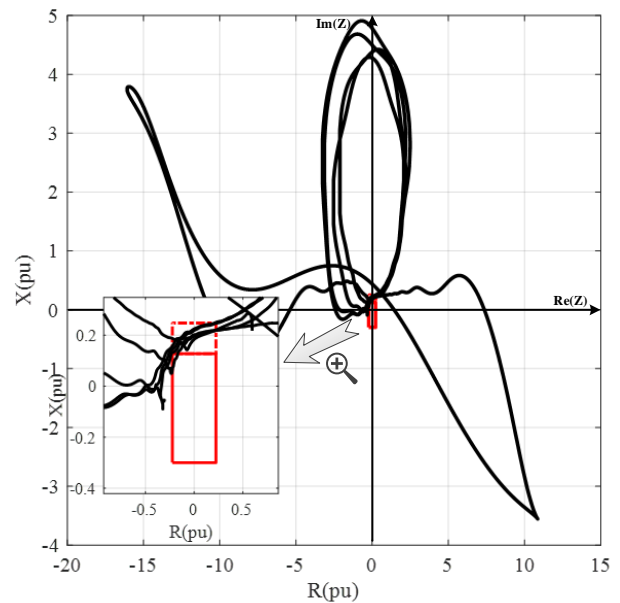


Fig. 17 Next rounds of impedance trajectory in the VR mode.

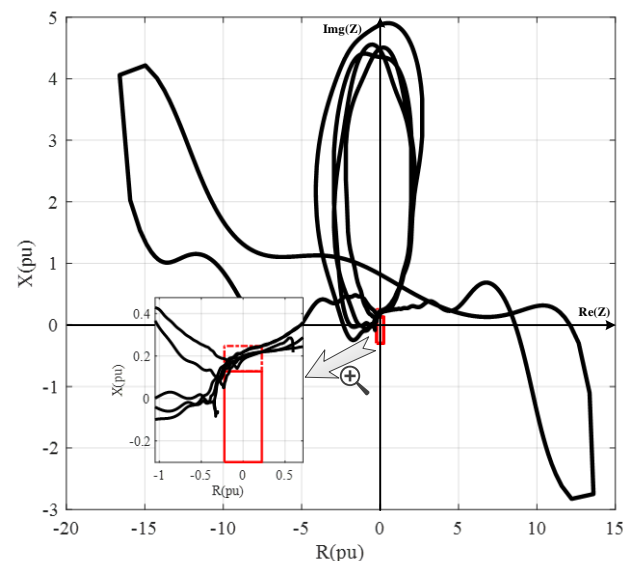


Fig. 18 The modified impedance trajectory in the QC mode.

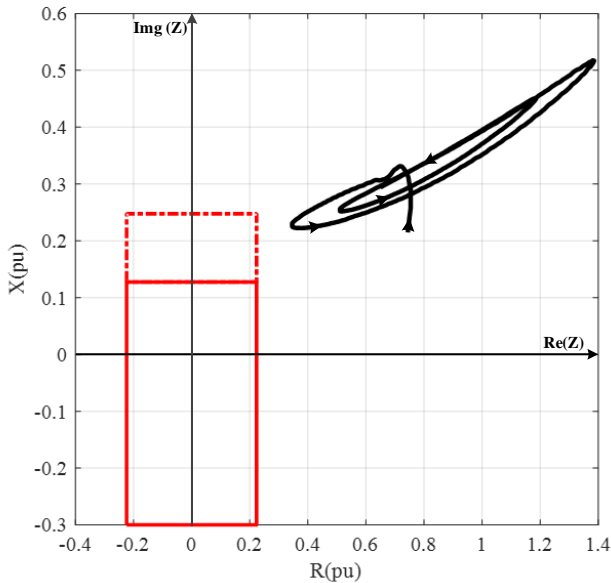


Fig. 19 The modified impedance trajectory in the stable rotor angle swing conditions.

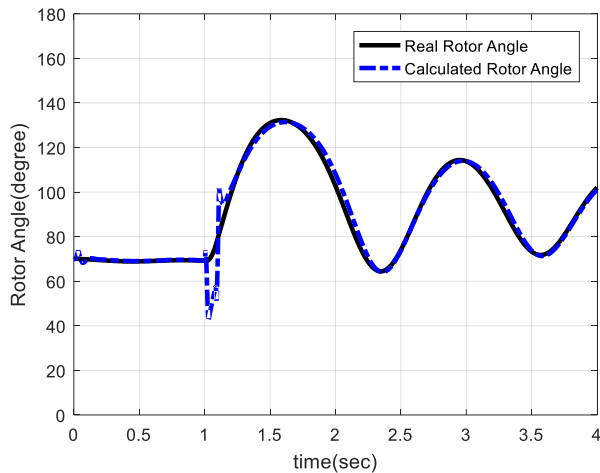


Fig. 20 The stable rotor angle swing after installing the STATCOM in the QC mode.

generalized into other shunt FACTS devices such as SVC, TCR, and FC-TCR. Given the speed of responding to the transitional conditions, each device will have different effects on OOS. New equations must be extracted for the series FACTS family. The only weakness of the approach presented in this paper is that it requires to receive phasor data from the remote bus/STATCOM bus. Nowadays, with the advent of the wide-area measurement system (WAMS), this possibility is provided by phasor measurement units. However, if the STATCOM installed in the power plant substation, the phasors data of STATCOM are available and it is not required to receive data by telecommunication.

### 5 Conclusion

In this paper, the effect of STATCOM on impedance-based OOS protection function has been investigated

and a novel modification function has been presented. The STATCOM with rapid response improves transient stability and increases critical fault clearing time. However, if the fault duration is greater than the critical fault clearing time, the generator will be unstable and the detection of relay will be disrupted. In this situation, both operation modes of voltage regulation and reactive power control of STATCOM cause the OOS to be not detected by the OOS relay. To solve this problem, an analytical adaptive approach is used to eliminate the effect of STATCOM. This approach requires remote bus voltage and current phasors to be sent to the relay location via the communication channel. Simulation results indicate that the presence of STATCOM changes the impedance path and interferes with the detection of the OOS relay. Also, the results demonstrate that the proposed modification improves the accuracy of OOS impedance-based function and help the correct diagnosis when the STATCOM is in service. Moreover, the modified function discriminates between stable and unstable power oscillations and the modified impedance path does not enter into the characteristic under stable power swing.

### Appendix 1

Table 1.1 Generator parameter.

Parameter	Value [p.u.]	Parameter	Value [p.u.]
$X_d$	1.81	$R_a$	0.003
$X_q$	1.76	$T'_{do}$	8.0
$X'_d$	0.30	$T'_{go}$	1.0
$X'_q$	0.65	$T''_{do}$	0.03
$X''_d$	0.23	$T''_{go}$	0.07
$X''_q$	0.25	$H$	3.5
$X_l$	0.15	$K_D$	0

### Appendix 2

A list of some sample system parameters of transformers and STATCOM:

**Transformers:**  $S_T = 2220$  MVA, 24/500 kV,  $R_1 = 0.002$ ,  $L_1 = 0$ ,  $R_2 = 0.002$ ,  $X_{L2} = 0.15$  p.u.,  $R_m = L_m = 500$  p.u., D1/Yg winding connection.

**STATCOM:** Nominal power =  $\pm 200$  MVA, Four phase shifting transformers:  $S_T = 200/4$  MVA and 125/24 kV,  $C_p = C_m = 3000$  F., Droop = 0.03, Voltage Regulator:  $K_P = 15$ ,  $K_i = 2500$ , VAr Regulator:  $K_P = 5$ ,  $K_i = 50$ .

### References

- [1] P. Kundur, *Power system stability and control*. New York: Mc-GrowHill, 1994.
- [2] B. Alinezhad and H. K. Kargar, "Out-of-Step protection based on equal area criterion," *IEEE Transactions on Power Delivery*, Vol. 32, No. 2, pp. 968–977, Mar. 2017.

- [3] P. M. Anderson, *Power System Protection Protective Schemes for stability enhancement*. New York, IEEE Press, 1998.
- [4] D. Reimert, *Protective relaying for power generation systems Loss of synchronism*. New York, CRC Press Taylor & Francis Group, 2006.
- [5] Y. Xue, T. Van Cutsem, and M. Ribbens-Pavella, "Extended equal area criterion justifications, generalizations, applications," *IEEE Transactions on Power Systems*, Vol. 4, No. 1, pp. 44–52, Feb. 1989.
- [6] V. Centeno, A. Phadke, A. Edris, J. Benton, M. Gaudi, and G. Michel, "An adaptive out-of-step relay," *IEEE Transactions on Power Delivery*, Vol. 12, No.1, pp. 61–71, Jan. 1997.
- [7] S. Paudyal, G. Ramakrishna, and M. S. Sachdev, "Application of equal area criterion conditions in the time domain for out-of-step protection," *IEEE Transactions on Power Delivery*, Vol. 25, No. 2, pp. 600–609, Apr. 2010.
- [8] S. Paudyal and R. Gokaraju, "Out-of-step protection for multi-machine power systems using local measurements," in *IEEE Eindhoven PowerTech*, Eindhoven, Netherlands, 2015.
- [9] M. McDonald, D. Tziouvaras, and A. Apostolov, "Power swing and out-of-step considerations on transmission lines," *IEEE PSRC WG D 6*, Jun. 2005.
- [10] E. Farantatos, G. J. Cokkinides, and A. P. Meliopoulos, "A predictive generator out-of-step protection and transient stability monitoring scheme enabled by a distributed dynamic state estimator," *IEEE Transactions on Power Delivery*, Vol. 31, No. 4, pp. 1826–1835, Aug. 2016.
- [11] N. G. Hingorani and L. Gyugyi, *Understanding FACTS: Concepts and technology of flexible AC transmission systems*. Piscataway, NJ: IEEE press, 2000.
- [12] A. Ghorbani, B. Mozafari, S. Soleymani, and AM. Ranjbar, "Operation of synchronous generator LOE protection in the presence of shuntFACTS," *Electric Power Systems Research*, Vol. 119, pp. 178–186, 2015
- [13] M. Khederzadeh and A. Ghorbani, "STATCOM modeling impacts on performance evaluation of distance protection of transmission lines," *European Transaction on Electrical Power*, Vol. 21, No. 8, pp. 2063–2079, Nov. 2011.
- [14] M. Khederzadeh and A. Ghorbani, "Impact of VSC-Based multiline FACTS controllers on distance protection of transmission lines," *IEEE Transactions on Power Delivery*, Vol. 27, No. 1, pp. 32–39, Jan. 2012.
- [15] T. S. Sidhu, R. K. Varma, P. K. Gangadharan, F. A. Albasri, and G. R. Ortiz, "Performance of distance relays on shunt-FACTS compensated transmission lines," *IEEE Transactions on Power Delivery*, Vol. 20, No. 3, pp. 1837–1845, Jan. 2005.
- [16] M. Khederzadeh and T. S. Sidhu, "Impact of TCSC on the protection of transmission lines," *IEEE Transactions on Power Delivery*, Vol. 21, No. 1, pp. 80–87, Jan. 2006.
- [17] X. Zhou, H. Wang, R. K. Aggarwal, and P. Beaumont, "The Impact of STATCOM on distance relay". in *15<sup>th</sup> PSCC*, Liege, pp. 22–26, Aug. 2005.
- [18] X. Zhou, H. Wang, R. K. Aggarwal, and P. Beaumont, "Performance evaluation of a distance relay as applied to a transmission system with UPFC," *IEEE Transactions on Power Delivery*, Vol. 21, No. 3, pp. 1137–1147, Jul. 2006.
- [19] F. A. Albasri, T. S. Sidhu, and R. K. Varma, "Performance comparison of distance protection schemes for shunt-FACTS compensated transmission lines," *IEEE Transactions on Power Delivery*, Vol. 22, No. 4, pp. 2116–2125, Oct. 2007.
- [20] A. Ghorbani, "Comparing impact of STATCOM and SSSC on the performance of digital distance relay," *Journal of Power Electronics*, Vol. 11, No. 6, pp. 890–896, 2011.
- [21] A. Ghorbani, B. Mozafari, and M. Khederzadeh, "Impact of SVC on the protection of transmission lines," *International Journal of Electrical Power and Energy Systems*, Vol. 42, No. 1, pp. 702–709, Nov. 2012.
- [22] M. Pazoki, Z. Moravej, M. Khederzadeh, and N. K. C. Nair, "Effect of UPFC on protection of transmission lines with infeed current," *International Transactions on Electrical Energy Systems*, Vol. 26, No. 11, pp. 2385–2401, 2016.
- [23] M. Elsamahy, S. O. Faried, and T. Sidhu, "Impact of midpoint STATCOM on generator loss of excitation protection," *IEEE Transactions on Power Delivery*, Vol. 29, No. 2, pp. 724–732, Apr. 2014.
- [24] A. Ghorbani, S. Soleymani, and B. Mozafari, "A PMU-based LOE protection of synchronous generator in the presence of GIPFC," *IEEE Transactions on Power Delivery*, Vol. 31, No. 2, pp. 551–558, Apr. 2016.
- [25] K. Raghavendra, S. P. Nangrani, and S. S. Bhat, "Modeling of operation of loss of excitation relay in presence of shunt FACTS devices," in *IEEE 6<sup>th</sup> International Conference on Power Systems*, pp. 1–6, 2016.

[26] H. Yaghoobi, "A new adaptive impedance-based LOE protection of synchronous generator in the presence of STATCOM," *IEEE Transactions on Power Delivery*, Vol. 32, No. 6, pp. 2489–2499, Dec. 2017.

[27] A. Esmaeilian, A. Ghaderi, M. Tasdighi, and A. Rouhani, "Evaluation and performance comparison of power swing detection algorithms in presence of series compensation on transmission lines," in *IEEE 10<sup>th</sup> International Conference on Environment and Electrical Engineering (EEEIC)*, Rome, pp. 1–4, 2011.

[28] P. Nayak, A. Pradhan, and P. Bajpai, "A fault detection technique for the series-compensated line during power swing," *IEEE Transactions on Power Delivery*, Vol. 28, No. 2, pp. 714–722, 2013

[29] Z. Moravej, M. Pazoki, and M. Khederzadeh, "Impact of UPFC on power swing characteristic and distance relay behavior," *IEEE Transactions on Power Delivery*, Vol. 29, No. 1, pp. 261–268, Feb. 2014.

[30] S. Jamali and H. Shateri, "Locus of apparent impedance of distance protection in the presence of SSSC," *International Transactions on Electrical Energy Systems*, vol. 21, No. 1, pp. 398–412, 2011.

[31] J. Khodaparast, M. Khederzadeh, FFD. Silva, and C. Leth Back, "Performance of power swing blocking methods in UPFC compensated line," *International Transactions on Electrical Energy Systems*, Vol. 27, No.11, p. e2382, 2017.

[32] A. G. Siemens, "Multifunctional Machine Protection 7UM62 Manual," 4.6 Ed., Siemens Co., pp. 165–174, 2010.

[33] M. A. Ghazizadeh and J. Sade, "New fault-location algorithm for transmission lines including unified power-flow controller," *IEEE Transactions on Power Delivery*, Vol. 27, No. 4, pp. 1763–1771, 2012.

[34] A. Ghorbani, S. Masoudi, and A. Shabani, "Application of the Posicast control method to static shunt compensators," *Turkish Journal of Electrical Engineering & Computer Sciences*, Vol. 20, No. 1, pp. 1100–1108, Jan. 2012.



**S. R. Hosseini** received the B.Sc. and M.Sc. degree in Electric Power Engineering from Zanzan University, Zanzan, Iran, and Isfahan University of Technology, Isfahan, Iran, in 2006 and 2009, respectively. Currently, he is pursuing the Ph.D. degree. His research interests include power system protection, flexible AC transmission systems devices, and power generation. His current research work is in wide-area power system protection and control.



**M. Karrari** received the Ph.D. degree in Control Engineering from Sheffield University, Sheffield, U.K., in 1991. Since 1991, he has been with the Amirkabir University of Technology, Tehran, Iran. He is author or coauthor of more than 100 technical papers and two books: *Power System Dynamics and Control*, 2004, and *System Identification*, 2012, all in Persian. His main research interests are power system modeling, modeling and identification of dynamic systems, and large-scale and distributed systems.



**H. Askarian Abyaneh** (SM'09) was born in Abyaneh, Isfahan, Iran, on March 20, 1953. He received the B.Sc. and M.Sc. degrees, both in Iran, in 1976 and 1982, respectively. He also received another M.Sc. degree and the Ph.D. degree from the University of Manchester Institute of Science and Technology, Manchester, U.K., in 1985 and 1988, respectively, all in Electrical Power System Engineering. He published over 100 scientific papers in international journals and conferences. Currently, he is a Professor with the Department of Electrical Engineering, Amirkabir University of Technology, Tehran, Iran, working in the area of the relay protection and power quality.



© 2019 by the authors. Licensee IUST, Tehran, Iran. This article is an open access article distributed under the terms and conditions of the Creative Commons Attribution-NonCommercial 4.0 International (CC BY-NC 4.0) license (<https://creativecommons.org/licenses/by-nc/4.0/>).